Thin Solid Films 548 (2013) 646–649

Contents lists available at ScienceDirect

Thin Solid Films

journal homepage: www.elsevier.com/locate/tsf

Morphological and electrical study of gold ultrathin films on mica

S. Bahamondes [a], S. Donoso [a], R. Henríquez [b], M. Flores [a,*]

[a] Departamento de Física, Facultad de Ciencias Físicas y Matemáticas, Universidad de Chile, Av. Blanco Encalada 2008, Santiago, Chile
[b] Departamento de Física, Universidad Técnica Federico Santa María, Av. España 1680, Valparaíso, Chile

ARTICLE INFO

Article history:
Received 20 December 2012
Received in revised form 29 August 2013
Accepted 30 August 2013
Available online 7 September 2013

Keywords:
Evaporation
Thin Films
Gold
Atomic force microscopy
Scanning tunneling microscopy

ABSTRACT

We present a topographical study of the formation of thin films of gold on muscovite mica. The characterization of the samples was done with scanning tunneling microscopy, atomic force microscopy as well as electric measurements. We performed our study on two groups of samples: first group of samples, evaporated at room temperature for thickness ranging from 1.5 up to 97 nm; second group of samples, for two different thicknesses of 3 nm and 50 nm evaporated at different substrate temperatures, between 110 and 530 K. The gold films show a Volmer–Weber growth. The complete films are obtained from samples with a nominal thickness of 8 nm deposited. The average grain diameter is constant, with nominal thicknesses of 18.5 nm, up to 8 nm and increases with the thickness for higher deposition. The average grain diameter is similar regardless of the temperature of the substrate for samples of 3 nm thickness, but changes for samples of 50 nm thickness. The resistivity is inversely dependent on nominal thickness and the mean free path is lineally dependent on nominal thickness.

1. Introduction

Polycrystalline ultrathin metal films have a huge importance in several fields of the materials science and nanotechnology [1]. In particular, the study of properties of thin metal film deposit onto insulated surfaces is very interesting for the development of electronic, magnetic and optical devices [2–4]. These properties are closely related to the microstructural characteristics of films such as crystalline structure, grain size, surface topography, etc. By changing any of these features is possible to adjust their properties, for example: electronic, magnetic and optical properties. In order to adjust the morphology of films, it is necessary to understand the mechanisms of formation of thin films and how these are influenced by the deposition conditions.

From the advent of the experimental techniques to create and characterize the surfaces the metallic thin films were explored a lot. Specially, gold thin films have been studied from the middle of the century [5,6], because it is easy to prepare by different deposition techniques, such as sputtering [7–13], resistive heating [3,4,14,15] or electron beam [6,16]. The resulting polycrystalline films are oriented, principally, in the [111] direction, over different substrates, crystalline [12,14,16] or amorphous [7,8]. Also, an ultra high vacuum system is not required for these studies, in fact some morphological characterizations are run in air [14], and also ex situ annealing can be performed in air [15]. In the nineties due to the easy preparation of the clean surfaces, the gold films were used to anchor organic molecules and self-assembled monolayers [17]. Nowadays, the focus moved to ultrathin gold island films. This is due mainly to the applications of these systems in plasmonic devices [3,4], where the preparation of the high quality thin films, prior to the thermal induction of the nanoislands, is very important. Also, due to its simplicity, this kind of films gives the possibility to study the charge transport [13,14]. The charge transport coefficients of the films are critically dependent on their morphology and their preparation, thereby providing information on those properties.

This paper presents a study on how the morphology of ultra thin and thin gold films evaporated onto mica at room temperature changes in function of their thickness (1.5 to 100 nm). Additionally, the effect of substrate temperature (110 to 540 K) was studied for two different thicknesses (3 and 50 nm). The morphology of the resulting films was characterized with atomic force microscopy (AFM) and scanning tunneling microscopy (STM). The electrical properties at 4 K were proved to depend on the film thickness.

2. Experimental details

Gold films of high purity (99.9999%) were deposited on freshly exfoliated Muscovite mica by physical method using a resistively heated tungsten basket. The mica shows a surface roughness 0.3 nm over areas of $1 \times 1\ \mu m^2$. A quartz balance located close to the sample monitored the thickness of the deposited film. Depositions were performed in a high vacuum system (10^{-4} Pa) and the evaporation rate used was 1.2 nm/min. While relatively low for this technique, such an evaporation rate allows a rearrangement of the atoms forming grains on the substrate [15]. Two series of samples were prepared. A first group consists of films of different thicknesses up to 100 nm keeping the substrate at room

* Corresponding author:
E-mail address: mflorescarra@ing.uchile.cl (M. Flores).

0040-6090/$ – see front matter © 2013 Elsevier B.V. All rights reserved.
http://dx.doi.org/10.1016/j.tsf.2013.08.104

temperature. The other group consists on films with thicknesses of 3 and 50 nm ranging the substrate temperature between 110 K and 540 K.

The substrate temperature during evaporation was adjusted by a homemade sample holder system, which was in thermal contact with a liquid nitrogen tank, for low temperature, and an electric oven, for high temperature [18]. The substrate temperature was monitored with a T-type thermocouple throughout the process.

The morphology of the gold film was characterized by scanning probe microscopy (SPM) at room temperature (RT). The SPM1 from Omicron operating in air was used. In the case of the non-conductive film the AFM contact mode was used, while for the conductive films the STM was used. The images were processed with a linear plane fit in order to remove the tilt before the statistical analysis with WSxM [19]. The average grain diameter was obtained by using the ImageJ software. This software was used to outline the grain perimeter, and then the diameter was estimated by assuming a circular surface which subtends the same area [14,20,21]. The statistical analysis was performed over 500 grains per sample, to ensure that such distribution is representative of the film observed [22].

Samples were placed in a copper block inserted in a superconducting magnet built by Janis Research Co. (Wilmington, MA, USA). The sample temperature was maintained at 4.2 ± 0.1 K. Transport measurements were performed using the 4-point method. The samples were fed a current of 0.5 mA and 210 Hz, voltage signals were acquired using computer controlled 830's LIA built by Stanford Research [18].

3. Results and discussion

A series of topographic images, obtained by SPM, of the gold films deposited at RT are shown in Fig. 1, for thicknesses ranging from 1.5 nm up to 97 nm. From the morphological characterization it is observed that the substrate is not completely coated up to 8 nm. Two stages are identified: (i) the substrate area recovered is lower than 70% and we mainly observe nucleation of islands, Fig. 1(a–c); and (ii) the area recovered is 100% and we mainly observe coalescence of grains, Fig. 1(d–h).

The gold deposited in the initial stage is organized in worm-like structures, without any preferential orientation. These structures are conformed by grains of approximately the same size, that ones are easily distinguished from the atomically flat mica [23]. For each thickness the grains were measured, characterizing its diameter and height, as well as the area coated, and the values are reported in Table 1. The results show how the coated area increases with the thickness deposited, while the grain size is constant. Such behavior implies that the growth dynamic favors the formation of grains to coat instead of the coarsening. The average height of the grain is h = 6.4 nm at t = 1.5 nm; this value is not modified by increasing the thickness, for example h = 6.8 nm at t = 3.0 nm. For thicker samples this behavior changes, for example at t = 6 nm the height is strongly increased, h = 10.5 nm, this value is consistent with the lower increment of the covered area, only 12% respect to t = 3.0 nm.

In the second stage, from 8 nm thick, the substrate is completely coated, Fig. 1(d). Ruffino et al. reported the same observation for a nominal thickness of approximately 28 nm [10,11], deposited by sputtering. We believe that this discrepancy is due to the different deposition techniques.

From t = 8 nm up to 97 nm we can observe the evolution of the grain size diameter, Fig. 1(d–g). This dependence is different for amorphous substrates [8,9]. From Tables 2 and 3, a different behavior of the mean grain diameter is observed, once gold covers complete the substrate.

From those series of images Volmer–Weber growth mode or 3D island formation [24] was evidenced, the diameter and height of the nanoislands were constant with the thickness, and in the range of thickness up to the continuous films is formed; in this stage the deposited material is nucleated forming structures over the percolation. For the lower coverage studied the nucleation stage is not observed, the deposited material coalesce forming worm-like structures. Similar structures were reported in Au onto amorphous Si_3N_4 [6], Pd films onto hexagonal SiC [9], Au films onto TiO_2(110) [25] and In film onto SiO_2 [26]. The formation of such structures was explained from the interrupted coalescence model [26]. But we obtain the dynamic scaling exponent, the graph is included in Fig. 2(a). In our case, the best fit of the experimental data give us a value z = 2.06; such value suggests the resistive evaporation of gold onto mica at room temperature and is in accordance with the nonequilibrium and nonconservative system. In the evolution of the gold grain the lateral growth is favored over the vertical growth. The covered area

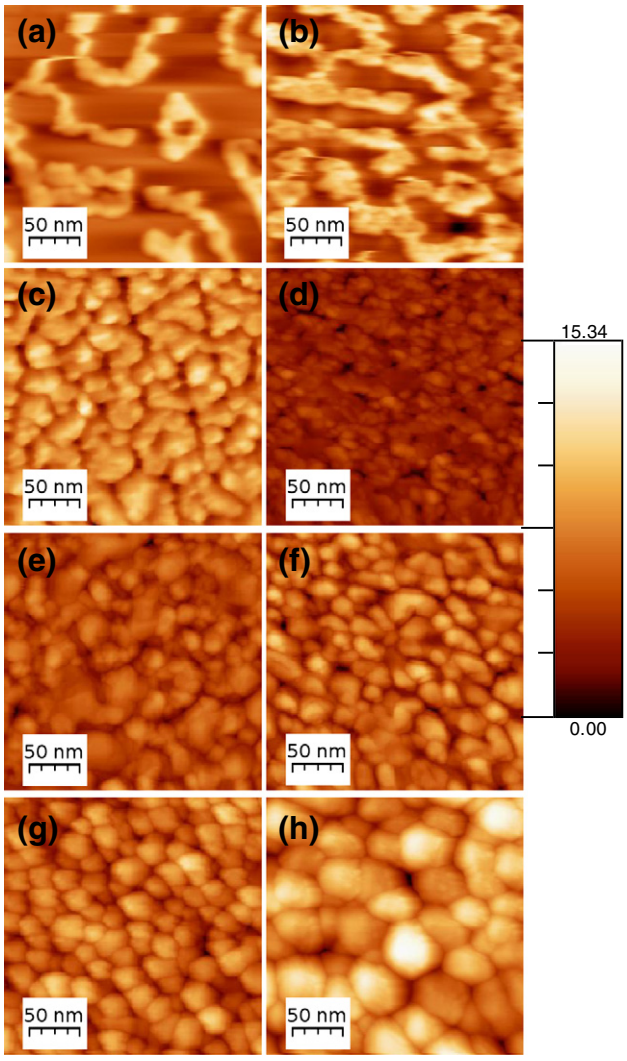

Fig. 1. Topographic image of thin gold films deposited at RT, for different thickness: (a) 1.5 nm, (b) 3.0 nm, (c) 6.0 nm, (d) 8.0 nm, (e) 17 nm, (f) 33 nm, (g) 50 nm and (h) 97 nm. The (a), (b) and (c) images were acquired by AFM. The remaining images, by STM. Area images of 250 nm × 250 nm.

Table 1
Morphological characterization of the samples for thickness 1.5, 3 and 6 nm, evaporated at room temperature. The morphological parameters represent the diameter d and its deviation Δ, island height h and covered area a.

t [nm]	d [nm]	Δ [nm]	h [nm]	a [%]
1.5	18.5	3.8	6.4	24
3	18.1	2.7	6.8	49
6	19.1	6.1	10.5	61

Table 2
Morphological and electrical characterizations of the samples from 8 up to 97 nm on thickness, evaporated at room temperature. The morphological parameters represent the diameter d, its deviation Δ, and island height h. The electrical parameters are the resistivity ρ and the mean free path L.

t [nm]	d [nm]	Δ [nm]	ρ (4 K) [nΩ m]	L(4 K) [nm]
8	10.7	3.0	70.9	11.8
17	15.3	8.4	42.1	19.9
33	18.6	6.8	28.0	29.8
50	23.7	6.9	14.5	57.7
97	38.0	13.7	6.65	125

was analyzed and included in Fig. 2(b), and the estimated Avrami factor was n = 1.06.

In order to determine the influence of the temperature in the grain formation, we fabricated two series of samples at different substrate temperatures: one for thickness that doesn't recover the substrate (3 nm) and the other that recover completely the substrate (50 nm). A series of topographical images, obtained by AFM contact mode, are shown in Fig. 3. They correspond to gold thin films of 3 nm thickness at different substrate temperatures during the evaporation: (a) 110 K, (b) 180 K, (c) 300 K and (d) 540 K. These samples show a uniformed coating and an agglomeration grains in worm-like structures for temperatures over RT, Fig. 3(b–d). Note that the samples deposited at temperatures below room temperature can be post-annealed by performing the AFM measurements at RT showing a slightly different topography [27]. The values of average grain diameter with their standard deviation, and the height characteristic at different temperatures are shown in Table 3. In contrast to the expected behavior, namely an inverse dependence of the characteristic height of the grains on the substrate temperature, the average grain diameter is similar for all samples.

This behavior can be understood based on a simple geometric model. We can assume that varying the substrate temperature does not change the volume of the grains; it might, nevertheless, change the contact area between the grain and the substrate. By increasing the substrate temperature a deformation occurs at the grain from ellipsoidal at truncated ellipsoidal. If the volume is considered approximately constant, then those would be a decrease in the height characteristic of 25% [16], and from our experimental results it is estimated at 28% reduction for extreme temperatures [21].

The values of the average grain diameter with their standard deviation along with the height characteristic at different temperatures in the 50 nm thick samples, are shown in Table 2. As in the samples 3 nm thick, the samples deposited at low temperatures can be annealed by measuring at RT. However, for this thickness, a different mean grain diameter appears in the samples deposited at temperatures below RT. This change for different substrate temperatures has been reported previously on gold films 50 nm thick on mica for substrate temperatures between 100 and 450 K [14]. These observations confirm that the formation of the film exhibits a different behavior before and after coating the substrate completely.

In the samples where the film covers completely the substrate, the resistivity was measured. The resistivity values appear in Table 2 and

Table 3
Morphological characterization of the samples for two different thickness t, 3.0 nm and 50 nm, evaporated at different substrate temperatures. The morphological parameters represent the island height h, diameter d and its deviation Δ.

Substrate temperature [K]	t ≈ 3 nm			t ≈ 50 nm	
	h [nm]	d [nm]	Δ [nm]	d [nm]	Δ [nm]
100–110	8.1	17.2	3.8	12.0	4.8
180	8.0	18.1	3.7	28.5	14.1
300	6.8	18.1	2.7	23.7	6.9
530–540	5.9	17.8	3.7	108	54.0

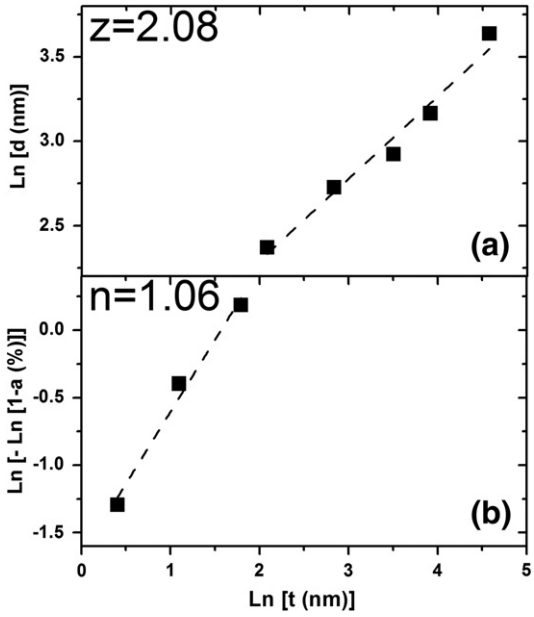

Fig. 2. (a) Diameter of the gold grains as a function of the film thickness in a log–log plot, the dotted line is the fit for z = 2.08. (b) Evolution of the covered area by the films as a function of the film thickness, the dotted line is the fit for n = 1.06.

are represented in Fig. 4(a). The line in the graph is added as eye guideline. To understand the electrical characterization, using the Drude's model, we obtained the mean free path L of electrons for each sample at 4 K [28,29]. From this model, the resistivity is defined by $\rho = \frac{m}{nq^2\tau}$; where m, n, q and τ are the mass, density, charge and scattering time of the electrons, respectively. The L was obtained from $L = \tau v_F$, where v_F is the Fermi velocity. The values of L(4 K) appear in Table 2, and are represented in Fig. 4(b). The results show a linear relation between L(4 K) and the thickness.

At 4 K, the phonons are frozen out, and then the resistivity at this temperature is controlled by the structural defects of the samples. So, these values allow complement of the structural characterization. Due to the resistivity and the grain size which are linearly dependent on thickness, we can establish a linear dependence between the resistivity

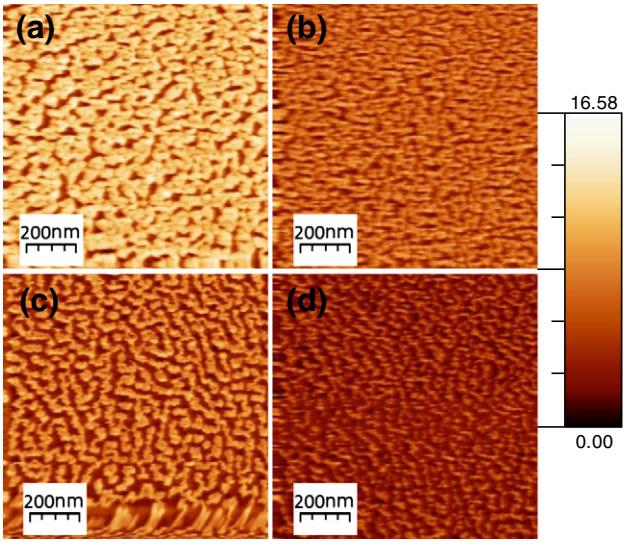

Fig. 3. Topographic image of thin gold films 3 nm thick, for different substrate temperatures: (a) 110 K, (b) 180 K, (c) 300 K and (d) 540 K. Area images of 1000 × 1000 μm^2 at F_n = 0.5 nN.

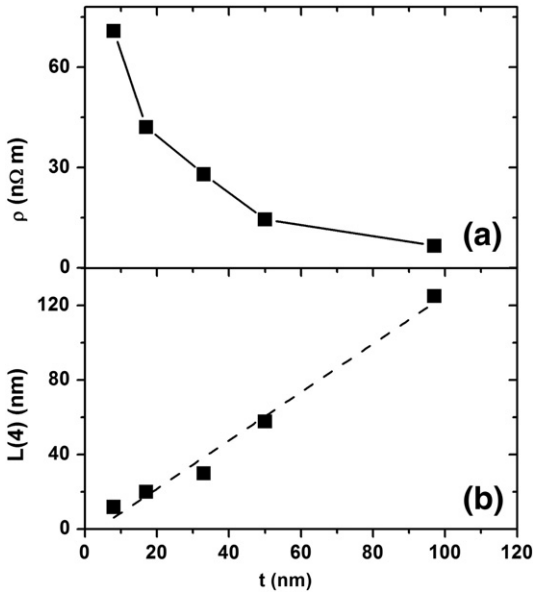

Fig. 4. Thickness dependence of (a) resistivity and (b) mean free path at 4 K.

and the grain size. From this point of view we infer that other scattering mechanisms, such as defects, are not introduced on the thin films as their thickness is increased.

4. Conclusions

The growth and formation of polycrystalline gold films onto mica were studied and the Volmer–Weber growth was observed. Initially the main grain diameter is constant up to 6 nm, when the substrate is not fully covered. In a second stage, the main grain diameter is linearly dependent on nominal thickness, at RT, from 8 nm. From this thickness upward the substrate is fully covered and the film is electrically continuous also. The resistivity is inversely dependent on nominal thickness and the mean free path is linearly dependent on nominal thickness.

Acknowledgment

We thank Professor A. S. Núñez for useful discussions. This work was partially supported by the projects PSD53, Fondecyt 11100277, and PIA Anillo ACT 1117. S. Bahamondes and S. Donoso give thanks for Conicyt Scholarship 22121149 and 22121141, respectively. R. Henriquez acknowledges funding from Proyecto Insercion CENAVA 791100037.

References

[1] H. Lüth, Solid Surfaces, Interfaces and Thin Films, Fifth edition Springer, 2010.
[2] N.G. Deshpande, M.S. Seo, X.R. Jin, S.J. Lee, Y.P. Lee, J.Y. Rhee, K.W. Kim, Appl. Phys. Lett. 96 (2010) 122503.
[3] A.B. Tesler, L. Chuntonov, T. Karakouz, T.A. Bendikov, G. Haran, A. Vaskevich, I. Rubinstein, J. Phys. Chem. C 115 (2012) 24642.
[4] H. Sun, M. Yu, G. Wang, X. Sun, J. Lian, J. Phys. Chem. C 116 (2012) 9000.
[5] H. Levinstein, J. Appl. Phys. 20 (1948) 306.
[6] R.F. Voss, R.B. Laibowitz, E.I. Allessandrini, Phys. Rev. Lett. 49 (1982) 1441.
[7] Z. Sun, J. Lü, X. Song, Vacuum 85 (2010) 297.
[8] V. Karoutsos, M. Toudas, A. Delimitis, S. Grammatikopoulos, P. Poulopoulos, Thin Solid Films 520 (2012) 4074.
[9] F. Ruffino, M.G. Grimaldi, F. Giannazzo, F. Roccaforte, V. Raineri, Nanoscale Res. Lett. 4 (2009) 262.
[10] F. Ruffino, V. Torrisi, G. Marletta, M.G. Grimaldi, Appl. Phys. A 100 (2010) 7.
[11] F. Ruffino, V. Torrisi, G. Marletta, M.G. Grimaldi, Nanoscale Res. Lett. 6 (2011) 112.
[12] W. Tang, K. Xu, P. Wang, X. Li, Microelectron. Eng. 66 (2003) 445.
[13] M.M. Yajadda, K.-H. Muller, K. Ostrikov, Phys. Rev. B 84 (2011) 235431.
[14] R. Henríquez, S. Cancino, A. Espinosa, M. Flores, T. Hoffmann, G. Kremer, J. Lisoni, L. Moraga, R. Morales, S. Oyarzún, M.A. Suarez, A. Zúñiga, R.C. Muñoz, Phys. Rev. B 82 (2010) 113409.
[15] I. Doron-Mor, Z. Barkay, N. Filip-Granit, A. Vaskevich, I. Rubinstein, Chem. Mater. 16 (2004) 3476.
[16] H. Hövel, I. Barke, Prog. Surf. Sci. 81 (2006) 53.
[17] C. Vericat, M.E. Vela, G. Benitez, P. Carro, R.C. Salvarezza, Chem. Soc. Rev. 39 (2010) 1805(and therein references).
[18] R. Henriquez, (Ph.D. thesis) Universidad de Chile, 2011.
[19] I. Horcas, R. Fernandez, J.M. Gomez-Rodriguez, J. Colchero, J. Gomez-Herrero, A.M. Baro, Rev. Sci. Instrum. 78 (2007) 013705.
[20] T. Sun, B. Yao, A. Warren, V. Kumar, S. Roberts, K. Barmak, K. Coffey, J. Vac. Sci. Technol. A 26 (2008) 605.
[21] S. Bahamondes, S. Donoso, R. Henriquez, G. Kremer, R. Muñoz, M. Flores, Av. Cien. Ing. 3 (2012) 79.
[22] G.R. Jones, M. Jackson, K. O'Grady, J. Magn. Magn. Mater. 193 (1999) 75.
[23] F. Ostendorf, C. Schmitz, S. Hirth, A. Kühnle, J.J. Kolodziej, M. Reichling, Nanotechnology 19 (2008) 305705.
[24] J.A. Venables, G.D.T. Spiller, M. Hanbücker, Rep. Prog. Phys. 47 (1984) 399.
[25] L. Zhang, F. Cosandey, R. Persaud, T.E. Madey, Surf. Sci. 439 (1999) 73.
[26] X. Yu, P.M. Duxbury, G. Jeffers, M.A. Dubson, Phys. Rev. B 44 (1991) 13163.
[27] C. Polop, C. Rosiepen, S. Bleikamp, R. Drese, J. Mayer, A. Dimyati, T. Michely, New J. Phys. 9 (2007) 74.
[28] P. Drude, Ann. Phys. 1 (1900) 566.
[29] N.W. Ashcroft, N.W. Mermin, Solid State Physics, Saunders College, New York, 1976. (Chap. 1).